

A GENERALIZED TOOL TO COMPUTE WAKE POTENTIAL AND IMPEDANCE FROM ELECTROMAGNETIC TIME DOMAIN SIMULATIONS

E. de la Fuente*, L. Giacomel, G. Iadarola, C. Zannini
CERN, Geneva, Switzerland

Abstract

An important problem in accelerators is the determination of the electromagnetic wakefields and their effect in the machine performance. These wakefields are generated inside the accelerator vacuum chamber due to the interaction of the structure with a passing beam. Among the properties that characterize their impact on the machine are the beam coupling impedance in frequency domain, and the wake potential in time domain. An accurate evaluation of these properties is crucial to effectively predict dissipated power and beam stability. This paper presents an open-source tool that integrates the electromagnetic (EM) wakefields for general 3D structures and computes the wake potential and impedance for longitudinal and transverse planes. Its usefulness is verified with the open-source EM-solver WarpX and benchmarked against the commercial software CST Studio.

INTRODUCTION

As the beam traverses the accelerator, it interacts with devices having different geometries (vacuum chamber, cavities, bellows) and materials with different EM properties (e.g. conductive or dielectric-coated pipes, magnets) [1]. These perturbations in geometry or EM properties generate electromagnetic fields known as *wakefields*. These wakefields are characterized by the term *wake*, as they cannot exist in front of the beam due to causality in the ultra-relativistic limit [2]. It is often useful to examine the frequency content of these fields using a Fourier transform, leading to the concept of *beam coupling impedance* [3] as introduced by V. G. Vaccaro in 1966.

The presence of beam coupling impedance can limit the accelerator's performance [4]. The interaction between the beam and wakefields can induce beam instabilities that lead to beam quality degradation, beam-induced heating and dynamic pressure spikes, compromising the functionality of some devices or machine's integrity. It is crucial to characterise the impedance of every accelerator component identifying which elements yield the largest contributions in the frequency range of interest. The single components are then assembled together building the total impedance model [5], which can be used in beam-dynamics codes [6, 7] to predict instabilities.

There are different methods to calculate the impedance of an accelerator element depending on its geometric and material features. Analytical calculations are possible for fairly simple geometries, such as tapered transitions [8, 9],

resonant cavities [10] and vacuum chambers made of lossy metals [11]. However, for arbitrarily shaped structures with a higher degree of complexity, impedance can only be obtained through numerical simulations, solving Maxwell's equations in time or frequency domain. These calculations are normally carried out with commercial codes, such as CST Studio [12], whose wakefield solver has been shown to agree well with bench measurements [13] and analytic predictions [14]. In this paper, we introduce the open-source Python tool Wakis [15], created to compute beam coupling impedance from pre-computed electromagnetic fields.

METHODOLOGY

EM wakefields are often characterized in time-domain by the *wake function*, which can be described as the electromagnetic response of a device to a pulse excitation (i.e., a point charge). If we consider a simple system of two charged particles, a source particle located at $\vec{r}_s = (x_s, y_s, z_s)$ and a test particle at position $\vec{r}_t = (x_t, y_t, z_t)$, the wake function $w(\mathbf{r}_s, \mathbf{r}_t, s)$ describes their electromagnetic coupling as a function of the distance s between them:

$$w(\mathbf{r}_s, \mathbf{r}_t, s) = \frac{1}{q_s q_t} \int_{-\infty}^{\infty} F_{\text{Lorentz}} dz. \quad (1)$$

The longitudinal beam coupling impedance is defined as the Fourier transform of the longitudinal wake function:

$$Z_{\parallel}(\omega) = \int_{-\infty}^{\infty} w_{\parallel}(\mathbf{r}_s, \mathbf{r}_t, s) e^{-i \frac{\omega s}{c}} \frac{ds}{c}. \quad (2)$$

The wake function cannot be obtained for a distributed source of charge (i.e., a particle beam) [16], but instead the wake potential $W(x_s, y_s, x_t, y_t, s)$ can be obtained as follows:

$$W(x_s, y_s, x_t, y_t, s) = \frac{1}{q_s} \int_{-\infty}^{\infty} dz [\mathbf{E}(x_s, y_s, x_t, y_t, z, t) + c \mathbf{e}_z \times \mathbf{B}(x_s, y_s, x_t, y_t, z, t)]_{t=\frac{s+z}{c}}. \quad (3)$$

In this setting, the beam charge distribution is considered the source \mathbf{r}_s , and \mathbf{r}_t corresponds to the integration path. The electric field will be affected by the relative position of the two. Note that for a non-ultra relativistic beam, one can use $v = \beta c$ in place of c . Since storing 3D maps of both electric and magnetic fields can be computationally challenging, it is common to split the wakefield into the longitudinal (\parallel , \mathbf{e}_z) and transverse (\perp , $\mathbf{e}_{x,y}$) components. In the longitudinal plane, the cross product cancels out, yielding:

$$W_{\parallel}(x_s, y_s, x_t, y_t, s) = \frac{1}{q_s} \int_{-\infty}^{\infty} dz E_z(x_s, y_s, x_t, y_t, z, t)_{t=\frac{s+z}{c}}. \quad (4)$$

* elena.de.la.fuente.garcia@cern.ch

The transverse contribution can be derived from the longitudinal wake potential using the Panofsky-Wenzel theorem [17]:

$$W_{\perp,\alpha}(s) = \frac{\partial}{\partial \alpha} \int_{-\infty}^s ds' W_{\parallel}(x_s, y_s, x_t, y_t, s'); \quad \alpha = x, y. \quad (5)$$

The beam coupling impedance can be calculated by the deconvolution of the wake potential $W_{\parallel}(s)$, $W_{\perp}(s)$, and the beam charge distribution $\lambda(s)$ in the Fourier space, using

$$Z_{\parallel}(\omega) = c \frac{\int_{-\infty}^{\infty} W_{\parallel}(s) e^{-i\omega s} ds}{\int_{-\infty}^{\infty} \lambda(s) e^{-i\omega s} ds}, \quad (6)$$

$$Z_{\perp}(\omega) = -ic \frac{\int_{-\infty}^{\infty} W_{\perp}(s) e^{-i\omega s} ds}{\int_{-\infty}^{\infty} \lambda(s) e^{-i\omega s} ds}. \quad (7)$$

To test the numerical algorithm implemented in Ref. [15] for the resolution of Eqs. (4-7), a simple model of a square pillbox cavity was used to obtain the electric field $E_z(x, y, z, t)$ along the integration path, using the CST Wakefield [12] solver and the PIC open-source code WarpX [18].

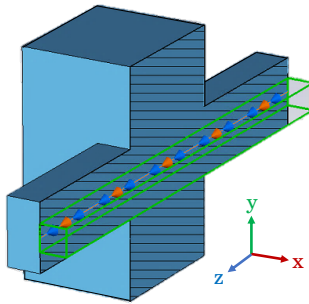


Figure 1: Longitudinal cut of the square pillbox cavity model used for the benchmark, showing the beam path (orange arrows) and integration path (blue arrows). The subvolume in which the E_z field was extracted is wire-framed in green.

The geometry of the rectangular pillbox cavity is shown in Fig. 1. The cavity is assumed to be made of perfect electric conductor (PEC). The domain boundary conditions are set to ‘PEC’ for both ends of x and y directions, and ‘open’ for both ends of z direction. The open boundaries apply a Perfect Matching Layer (PML) in order to absorb the outgoing EM waves. The beam moves along the z axis at the speed of light and its longitudinal distribution is Gaussian, with RMS size $\sigma_z = 5$ cm. Mesh refinement studies were carried out to ensure good convergence of the EM solvers.

RESULTS

To test the numerical algorithm, the electric field $E_z(x, y, z, t)$ was extracted in a sub-volume centered at the beam path (z -axis) with a width of at least 6 mesh cells in x and y directions. In order to achieve the maximum possible accuracy, the field is saved at every simulation time step (in CST this is achieved using a *Field Monitor*). In the CST Wakefield solver, the simulated wake length W_l is set

to 10 m. To achieve the same in WarpX, one needs to set the maximum simulation time to

$$t_{max} = (W_l + (z_{max} - z_{min}) + 2n_{pml}\Delta z)/c + t_{inj},$$

where $n_{pml} = 10$ is the thickness of the PML in number of cells, and t_{inj} is the time needed for the beam to enter the simulation domain. In CST, we empirically found $t_{inj} = 8.54\sigma_z/c$. Note that, since in WarpX simulations the beam is injected at the center of the PML region, an extra $(n_{pml}/2)\Delta z/c$ needs to be added to t_{inj} in order to match the CST simulation time.

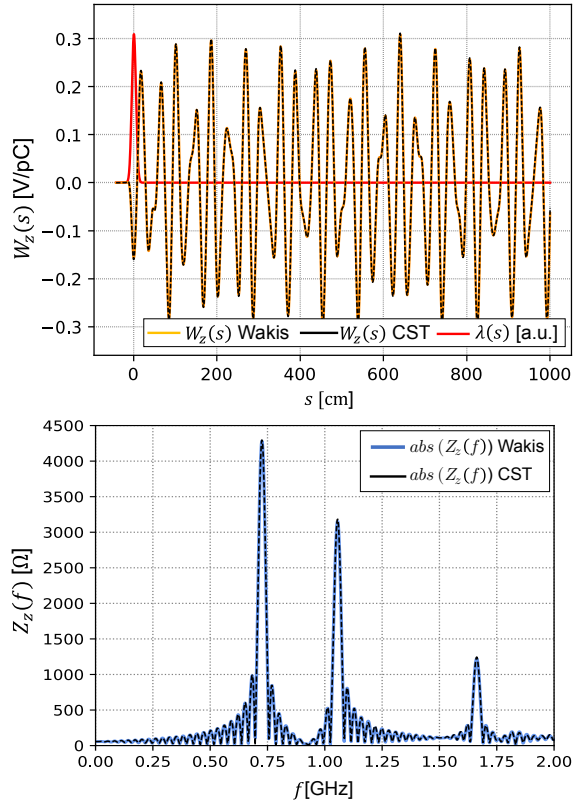


Figure 2: Longitudinal wake potential (top) and beam coupling impedance (bottom) for a pillbox cavity, obtained by Wakis using Eq. (4) on CST solver’s E_z field and compared with CST Wakefield solver results.

In post-processing, one can obtain the longitudinal wake potential from the saved E_z field maps using Eq. (4). Note that the E_z field is evaluated in time at $t = (s + z)/c$, which depends on the integration variable z . The wake is computed at discrete values of s from $s_{min} = -t_{inj}c$ to $s_{max} = W_l$ spaced by $\Delta s = c\Delta t$. For every discrete value of s , one needs to integrate E_z from z_{min} to z_{max} , and for every t in the window

$$t_k = (z_k + s_n)/c - z_{min}/c + t_{inj}, \quad \forall z_k \in \{z_{min}, \dots, z_{max}\}.$$

As shown in Fig. 2 (top), the algorithm implemented in Wakis agrees well with CST. The normalized charge distribution $\lambda(s)$ is included on top of the wake potential to

enhance the understanding of the wake length dimensions. The beam coupling impedance is obtained using the same frequency analysis as in CST: a 1000 samples single-sided FFT. In Wakis we use the `fft` routine of the `numpy` package, on both the charge distribution and the wake potential. The maximum frequency can be defined by the beam σ_z , using $f_{max} = c/3\sigma_z$ as an empirical rule. The absolute value of the obtained longitudinal impedance is shown in Fig. 2 (bottom). Outstanding agreement between Wakis and the CST Wakefield solver is achieved.

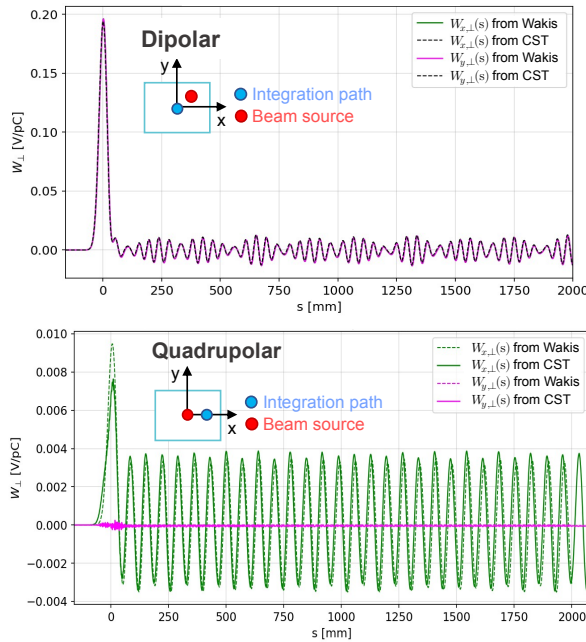


Figure 3: Transverse dipolar (top) and quadrupolar (bottom) wake potential for a pillbox cavity, obtained by Wakis using Eq. (5) on CST solver's E_z field and compared with the wake potential given by CST Wakefield solver.

One can expand the transverse wake potential as [19]

$$W_{\perp,x}(x, y, s) = W_{Cx}(s) + W_{Dx}(s)\Delta x_s + W_{Qx}(s)\Delta x_t + \mathcal{O}(x^2),$$

where the zero-th order induces an orbit offset for asymmetric structures, W_{Dx} is the dipolar term and W_{Qx} is the quadrupolar term. In our Python tool, the transverse wake potential and impedance are computed through Eq. (5). The gradient is calculated using a second-order central finite difference scheme. Depending on the relative displacement of the beam and the integration path, one can obtain the dipolar or quadrupolar wake potential. Results are shown in Fig. 3, where the displacement of the beam and integration path is depicted in a small schema. Note that for the dipolar case, since the displacement of the beam is diagonal, W_x and W_y are overlapping. The quadrupolar result shows a higher discrepancy due to the limited transverse resolution of the E_z field component extracted from CST.

The electromagnetic PIC solver WarpX was benchmarked against CST Studio, as a possible open-source alternative for

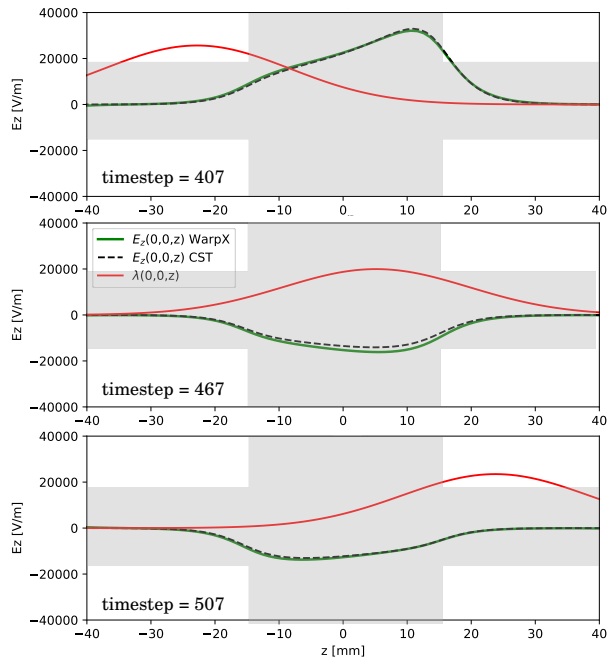


Figure 4: Comparison between both WarpX and CST $E_z(0, 0, z, t)$ fields as the beam $\lambda(z)$ traverses the cavity, for different time steps. The longitudinal section of the pillbox cavity is depicted shaded in grey.

Wakefield simulations. Results for the E_z field are displayed in Fig. 4, showing a very good agreement. Wake potential and impedance results using WarpX+Wakis combination are also in very good agreement with CST Wakefield solver, as presented in Ref. [20].

CONCLUSIONS

An open-source Python package, Wakis [15], was developed in order to obtain longitudinal and transverse wake potential and impedance from pre-computed EM fields. The algorithm has been benchmarked against the CST Wakefield solver [12] using a simple model of a pillbox cavity for the longitudinal, transverse dipolar and transverse quadrupolar cases. The two solvers are in excellent agreement. The WarpX PIC solver [18] has been explored as an alternative, open-source EM solver for wakefield simulations with PEC material boundaries. The E_z field has been benchmarked against CST particle studio. Work is ongoing to fine-tune WarpX simulations and test its performance in more complex devices.

REFERENCES

- [1] E. Métral, "Impedance theory and modeling," *CERN Yellow Rep. Conf. Proc.*, vol. 1, pp. 69–76, 2018.
doi:10.23732/CYRCP-2018-001
- [2] A. Chao, *Physics of Collective Beam Instabilities in High-Energy Accelerators*. John Wiley & Sons, 1993. <https://www.slac.stanford.edu/achao/wileybook.html>

- [3] V. G. Vaccaro, "Longitudinal instability of a coasting beam above transition, due to the action of lumped discontinuities," CERN, Internal Report ISR-RF/66-35, 1966. <https://cds.cern.ch/record/1216806>
- [4] B. Salvant, "Impedance and Instabilities in Hadron Machines," *CERN Yellow Rep. Conf. Proc.*, vol. 1, pp. 99–103, 2018. doi:10.23732/CYRCP-2018-001.99
- [5] B. Salvant *et al.*, "Building the Impedance Model of a Real Machine," in *Proc. IPAC'19*, Melbourne, Australia, May 2019, pp. 2249–2254. doi:10.18429/JACoW-IPAC2019-WEYPLS1
- [6] N. Mounet, *DELPHI: an Analytic Vlasov Solver for Impedance-Driven Modes*, CERN-ACC-SLIDES-2014-0066, 5 July 2014. Available at: <https://cds.cern.ch/record/1954277>.
- [7] A. Oeftiger, *An Overview of PyHEADTAIL*, CERN-ACC-NOTE-2019-0013, 23 April 2019. Available at: <https://cds.cern.ch/record/2672381>.
- [8] G. Stupakov, "Low frequency impedance of tapered transitions with arbitrary cross sections," *Phys. Rev. ST Accel. Beams*, vol. 10, p. 094401, 2007. doi:10.1103/PhysRevSTAB.10.094401
- [9] V. Smaluk, R. Fielder, A. Blednykh, G. Rehm, and R. Bartolini, "Coupling impedance of an in-vacuum undulator: Measurement, simulation, and analytical estimation," *Phys. Rev. ST Accel. Beams*, vol. 17, p. 074402, 2014. doi:10.1103/PhysRevSTAB.17.074402
- [10] T. Suzuki, "On the Coupling Impedance of a Resonant Cavity," in *Proc. PAC'81*, Washington D.C., USA, Mar. 1981, pp. 2566–2568.
- [11] K. Yokoya, "Resistive wall impedance of beam pipes of general cross section," *Part. Accel.*, vol. 41, pp. 221–248, 1993. <https://cds.cern.ch/record/248630>
- [12] *CST Particle Studio*, <https://www.cst.com/>.
- [13] A. Kurtulus *et al.*, "Detailed Electromagnetic Characterisation of HL-LHC Low Impedance Collimators," in *Proc. IPAC'21*, Campinas, Brazil, May 2021, pp. 4258–4261. doi:10.18429/JACoW-IPAC2021-THPAB235
- [14] C. Zannini, N. Mounet, E. Métral, G. Rumolo, and B. Salvant, "Electromagnetic Simulations of Simple Models of Ferrite Loaded Kickers," in *Proc. IPAC'10*, Kyoto, Japan, May 2010, pp. 2045–2047. <http://accelconf.web.cern.ch/IPAC10/papers/TUPD052.pdf>
- [15] E. de la Fuente Garcia, *Wakis: Wake and Impedance Solver*, <https://github.com/ImpedanCEI/wakis/>.
- [16] T. Weiland and R. Wanzenberg, "Wake fields and impedances," *Lect. Notes Phys.*, vol. 400, pp. 39–79, 1992. doi:10.1007/3-540-55250-2_26
- [17] S. Vaganian and H. Henke, "The Panofsky-wenzel Theorem And General Relations For The wake Potential," *Part. Accel.*, vol. 48, pp. 239–242, 1995. <https://cds.cern.ch/record/1108316>
- [18] Berkeley Lab, *WarpX: A Particle-In-Cell Code for Plasma Simulations*, <https://github.com/ECP-WarpX/WarpX/>. <https://warpx.readthedocs.io/en/latest/>
- [19] G. Rumolo, "Beam Instabilities," 2014, Comments: 21 pages, contribution to the CAS - CERN Accelerator School: Advanced Accelerator Physics Course, Trondheim, Norway, 18-29 Aug 2013. doi:10.5170/CERN-2014-009.199
- [20] E. de la Fuente, *Wakis (in-house wake and impedance solver)*, Presented at CERN ABP Group Information Meeting, 28th April 2022. Available at: <https://indico.cern.ch/event/1154158/>.